OPTOELECTRONICS AND ADVANCED MATERIALS – RAPID COMMUNICATIONS Vol. 4, No. 12, December 2010, p. 2032 – 2038

Effect of the morphology on the optical and electrical properties of TPyP thin films deposited by vacuum evaporation

M. SOCOL*, O. RASOGA, F. STANCULESCU[a], M. GIRTAN[b], A. STANCULESCU
National Institute of Materials Physics, 105 bis Atomistilor Street, P.O. Box MG-7, 077125, Bucharest-Magurele, Romania
[a]*Faculty of Physics, University of Bucharest, Str. Atomistilor nr.405, P.O.Box MG-11, Bucharest-Magurele, 077125 Romania*
[b]*Laboratoire de Photonique d'Angers, Université d'Angers, 2, Bd. Lavoisier, 49045, Angers, France*

We have studied the effect of the morphology on the optical and electrical properties of the TPyP thin films deposited by vacuum evaporation on different substrates (Si with different characteristics, ITO, quartz and glass). The presence of some well-defined B and Q absorption bands has been evidenced. FTIR and photoluminescence measurements have been used to confirm the preservation of the chemical structure of the compound during the evaporation process. The contact Au/TPyP/Si(n) is rectifier, while a blocking behavior has been shown by Si(n)/TPyP/Si(n) and ITO/TPyP/Si(n) and an injector dominated behavior by Si(p)/TPyP/Si(p) and ITO/TPyP/Si(p) heterostructures. The best transmission was obtained on TPyP film deposited on ITO and the highest value of the current in heterostructures Si(n) electrode characterised by a large grain morphology and in consequence by a weak optical and charge carrier scattering at the grain boundaries.

(Received November 18, 2010; accepted November 29, 2010)

Keywords: TPyP, Thin film, Morphology, Heterostructure

1. Introduction

Lately an increased interest was paid to the study of porphyrines because their show a strong optical absorption in visible region of the solar spectrum, which can have application in opto-electronics for OLEDs as n type conduction layer, in medicine as photosensitizers in photodynamic therapy and in photovoltaics as inexpensive materials for solar cells [1; 2; 3]. The basic structure of porphyrin consists of four pyrrolic entities kinked by four unsaturated methine bridges. The skeleton has un extended π-conjugated system with a large number of π-electrons leading to a wide spectral range for light absorption.

A special attention is focus on the meso-substituted porphyrines showing special functionality correlated with the meso-substituents named legs which are able to rotate at different dihedral angles around the C-C, σ bounds that connect the substituents to the porphyrine core, allowing the conformational adaptation of the molecule to the substrate [4, 5]. The phorphyrine core, which is usually planar, can be distorted as a result of the steric repulsion between the hydrogen atoms of the ring and the hydrogen atoms of the phorphyrine macrocyclem [6, 7].

Porphyrins have attracted much interest due to their interesting optical and electronic properties and to the possibility of tailoring their properties by molecular engineering [4].

Porphyrins and their derivatives are an ubiquitous class of natural compounds having biological importance such as chlorophyll, hemes and vitamins B_{12} [8, 9].

The organic semi-conductor 5,10,15,20-tetra(4-pyrydil)21H,23H-porphyne (TPyP) is a non-metallic porphyrine and as all the metal free or metal porphyrines is characterized by a n-type conduction own to the pyridyl groups replacing the phenyl groups resulting in an increase in the electron affinity. The N termination of the lateral groups favors the link to metal centers [5].

Recent studies have revealed that the surface morphology plays a key role in modifying the electrical properties of the junction. Therefore the investigation of the correlation relationship between morphology and optical and electrical properties is of great importance in the development of organic devices with tailored performances.

This paper presents some results related to the effect of the morphology evaluated by AFM measurements on the properties of the TPyP films deposited by vacuum evaporation on different substrates. The surface roughness evaluated from AFM measurements has influenced the optical properties of the films and electrical conduction through the heterostructures based on TPyP films.

2. Experimental

Thin films of TPyP have been prepared by vacuum evaporation and deposition on quartz, Si and ITO covered glass substrates with rectangular geometry. The double side etched Si wafers "p" type, resistivity ρ=3 Ωcm, "n" type resistivity ρ=17 mΩcm were successively cleaned with acetone, hydrofluoric acid and distillate water. ITO/aluminosilicate glass (5-15 Ω/□**),** quartz and glass platelets were cleaned with acetone.

We have used an Alcatel system with turbo molecular pump for the evaporation of organic powder and deposition of stable, homogeneous films characterized by a good adhesion to the substrate. The powder is introduced in a quartz crucible, which is introduced into a self-sustainable kanthal winding. The flux of molecules is limited and oriented to the substrates holder by a glass cylinder. Details about the experimental configuration have been previously presented [10, 11]. During the deposition process the pressure varied in the chamber between 1.5×10^{-5} mbar and 2×10^{-5} mbar. The evaporation temperature measured with a thermocouple situated at the bottom of the crucible was of 175-185 ^{o}C.

Subsequently, sandwich type SIS heterostructures, have been prepared putting into direct contact the organic layer of the structures Si/TPyP and Si/TPyP and Si/TPyP and ITO/TPyP. A special type of structure was prepared on glass substrate using a special grid configuration of the Al electrodes deposited by vacuum evaporation. The Au contact was deposited by sputtering on ITO/TPyP and p and n Si/TPyP samples.

The transmission spectra at room temperature have been recorded with a UV-VIS-NIR Carry 5000 Spectrophotometer and the photoluminescence spectra with a Edinburg Instruments FS-900 Spectrofluorimeter (experimental conditions: $\lambda_{excitation}$=435 nm; measurement range=450-850nm; slit 3.5; 3.5; step 1; integration time 0.25 s).

A MultiView 4000 Nanonics configuration based on an Olympus BX51 dual microscope has been used to obtain information on the topographic and optical image of the films. The optical microscopy remains an important investigation tool because it can be performed under ambient conditions without special preparation of the sample. We have obtained the AFM image with the microscope working in non-contact mode and the SNOM image with the microscope working in reflection mode. SNOM technique is proposed to surpass the fundamental limitation in spatial resolution due to the diffraction limit, which is approximately half the wavelength of the light used for sample illumination. SNOM is a kind of scanning probe microscopy where the surface of the sample is scanned with a nanometre scale light emitter placed in close proximity of the surface at a distance smaller than the wavelength of light. Light source is a Nd:YAG laser (λ=532 nm, P_{max}=20mW) coupled to a cantilevered monomode fiber probe with the following characteristics: Cr/Au coating, $\nu_{resonance}$=37 kHz, $\phi_{aperture\ diameter}$=100 nm and active quality factor in phase feedback Q =680. The scattered light is collected by a 50X objective and sent to a high gain photomultiplier tube, MP-942 Perkin-Elmer with a spectral response between 165-650 nm.

To draw the I-V characteristics of these heterostructures we have used a perpendicular configuration with 4 wires contact geometry to eliminate the effect of the contacts. The structure is connected to a Keithley 2400 SourceMeter. Because the currents passing through organic structures are small being limited by the small mobility of the charge carriers in organic semiconductors, the effect of the external perturbations has been limited by the special metallic isolation box.

The resistivity of the silicon wafers has been measured using the standard in-line four-point probes configuration.

3. Results and discussions

The absorption spectra of the porphyrins show a special feature characterized by the presence of some well-defined absorption bands situated in different spectral regions denoted as Q, B, N, L and M bands [12, 13]. The Q band consists in 4 bands situated in visible (500-700 nm), the band B (Soret) situated between 350-500 nm and the bands L, N and M are situated in UV.

The UV-Vis transmission spectra of the TPyP thin films have evidenced a structured shape of the transmission curve in the domain ranging from 200 nm to 800 nm. It shows the π-π* absorption bands characteristic of free-base ethio type porphyrin, which are associated with π-π* transition between bonding and anti-bonding molecular orbitals. An intense Soret band (B) with a peak around 430 nm and 4 Q bands situated at 520 nm, 555 nm, 590 nm and 645 nm have been evidenced (Fig. 1). The absorption spectra play an important role to determine optimum illumination of the solar cell and then to increase the efficiency.

The shape of the absorption spectra of the thin films deposited by vacuum evaporation on different substrates is preserved for wavelengths > 430 nm (Fig. 1). No absorption band have been observe in UV for TPyP film deposited on quartz (Fig. 1a). Some differences have been evidenced for TPyP film deposited on ITO covered glass. The Soret band situated at 430 nm it is not very well structured and seems to disappear (Fig. 1c), while a weak UV absorption peak appeared around 330 nm. The slight red shift of the B band is determined by the interaction between the molecules in the solid state.

This behavior can be correlated with the particularities of the organic layer, the electronic and optical properties of the molecular architecture depending on the characteristics of the individual molecules as the building blocks of the layer and on the type of connection existing between the molecules in the vacuum deposited layer [4].

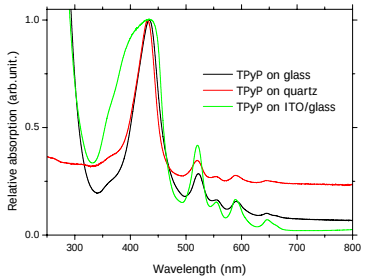

Fig. 1. UV-VIS absorption spectra of TPyP thin film deposited by vacuum evaporation on different substrates (quartz, glass, ITO).

Conformation of TPyP is defined by several degrees of freedom: dihedral angle describing the rotation of a pyridyl group about the C-C bond, connecting it to the porphyrin core, inclination angle that indicates the inclination of the same C-C bond out of the macrocycle plane towards the surface and a distortion angle. The steric repulsion between hydrogen atoms of the pyridyl ring and of the pyrrole moieties can lead to the distortion of the macrocycle [14].

The molecules are centered on "bridge" sites of the substrate and can exhibit a strong deformation involving a saddle-shaped macrocycle distortion as well as considerable rotation and tilting of the meso-substituents. A possible bonding mechanism can be based on the pyridyl−surface interaction, which mediates the molecular deformation upon adsorption on the substrate's surface [15]. This can be a hydrogen bond between the N from pyridyl and O dangling bond on the ITO surface, which are beneficial for the initial nucleation of TPyP and subsequent growth of the film.

Subsequent molecule packing could be due to the non-covalent interactions mediated by the terminal pyridyl groups and intermolecular interactions seem to prevail over site-specific adsorption. For the optimization of the intermolecular interactions the porphyrin core can be severely deformed and the symmetry of the molecule can be modified.

The four pyridyl substituents of TPyP contain a terminal nitrogen lone pair, which is reactive towards the O dangling bonds on ITO surface. These interactions affect the conformational structure and, as a result, the local symmetry in the deposited layer, with effect on the allowed transitions reflected in the UV-VIS spectrum.

The Soret band have disappeared and new L band has appeared because the associated transitions have become forbidden and other transitions allowed from these symmetry change as a result of saddle-shape distortion where 2 pyrrole rings are bent up and 2 are bent down [14].

Quartz substrate doesn't show dangling bonds because the valence is satisfied in the elementary cell compared to ITO where the presence of the dangling bond is associated with the nonstoichiometry of the layer. For this reason the shape of the abs curve is similar for quartz and glass substrates.

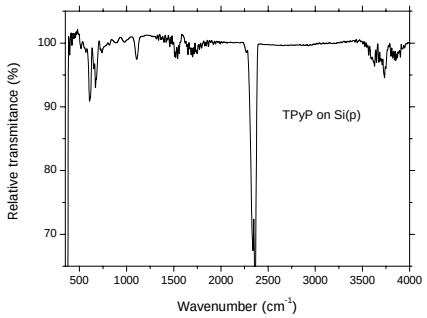

Fig. 2. FTIR spectra of TPyP film on p type Si substrate.

The FTIR spectra of solid state TPyP is in agreement with the FTIR spectra of powder BrK mixture [2]: the absorption at 3306 and 975 cm^{-1} correspond to stretching and bending vibrations of N-H and C-N respectively characteristic for the absorption of the porphyrin free base; the absorption bands in the range 1500-1600 cm^{-1} are generated by the stretching vibration of C=C in the pyridyl aromatic ring; the intense absorption band situated at 798 cm^{-1} is generated by the vibration of C-H bond from pyrrole.

This means that by vacuum evaporation the chemical structure is preserved and this is an adequate method for the preparation of TPyP thin films.

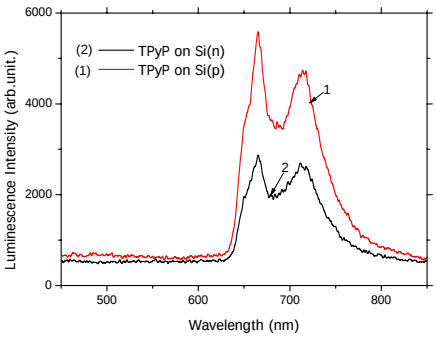

Fig. 3. Photoluminescence spectra of TPyP film on Si p type (1) and Si n type (2).

The photoluminescence spectra of TPyP films deposited on Si have revealed two emission Q bands situated at 660 nm and 710 nm which correspond to free base TPyP (2).

The surface morphology of the thin films of TPyP deposited on different substrates was analyzed were performed by comparing, for a given substrate, the topographic information obtained by AFM with the optical image of the layer obtained by Near Field Scanning Optical Microscopy (NSOM).

For the evaluation of the layer roughness, RMS (root mean square) and RA (roughness average) parameters as well as the peak to peak) heights (vertical scale) have been determined.

The morphology characterized by large grain dimension and decrease in surface area can be responsible for better transmission properties (for optical transparent substrates) because of the reduction in the scattering taking

place at the grain boundaries [16, 17]. This morphology can also enhance the electrical transport (for conductor substrates) [16, 17]. The shape and size of the grains depends on the deposition conditions and type of substrate.

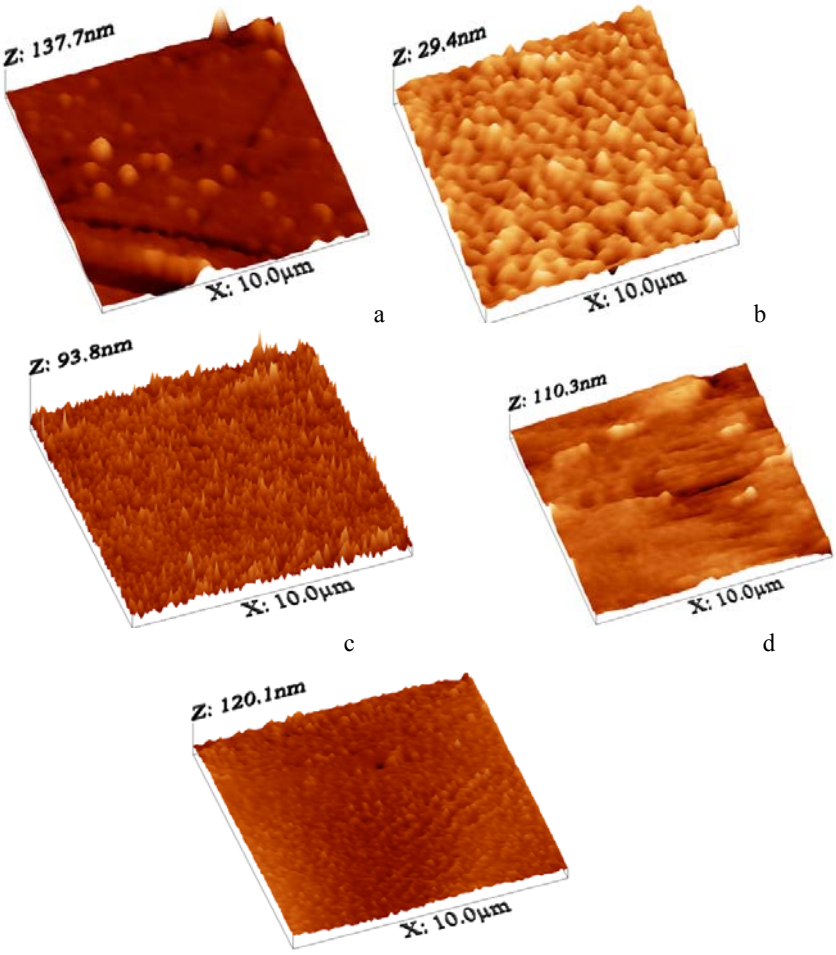

Fig. 4. AFM images on TPyP thin films deposited on different substrates: (a) glass; (b) ITO; (c) quartz; (d) Si type p; (e) Si type n.

Table 1. RMS, RA for TPyP film grown by vacuum evaporation on different substrates.

Sample	RMS (nm)	RA	Verticale scale
TPyP/glass	8.95	5.4	137.7
TPyP/ITO	2.37	1.8	29.4
TPyP/quatz	9.22	7.14	93.7
TPyP/Si(p)	9	6.58	110
TPyP/Si(n)	9.93	7.43	120

Because the sample are deposited in the same experimental conditions, the higher values of RMS and RS for the sample prepared on quartz compared to glass and ITO (Table 1) are associated with a large grain morphology (Fig. 4 a and Fig. 4 b) that implies a decreasing of the scattering at the grain boundaries in the succession: TPyP/quatz<TPyP/glass/TPyP/ITO.

On the other hand, the TPyP layer grown on n type Si is characterized by higher values for RMS and RA (Table 1) compared to the layer grown on p type Si. As a consequence the large grain morphology of TPyP/Si(n) (Fig. 4c and Fig. 4 d) sustains a lower charge carriers scattering in these samples and higher values for the injected currents.

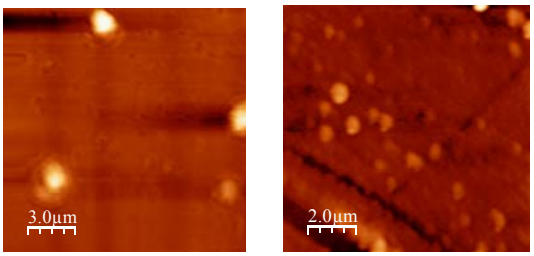

Fig. 5. Comparative image of TPyP film deposited on glass substrate obtained by (a) NSOM; (b) AFM.

The grain morphology of the TPyP film deposited by vacuum evaporation on glass substrate was confirmed by the NSOM image of the film obtained (Fig. 5).

The electrical transport properties of the heterostructures Si(p)/TPyP/Si(p) and Si(n)/TPyP/Si(n) are different. For applied voltages <0.5 V, at direct and

reverse polarization, the Si(n)/TPyP is a blocking contact (Fig. 6 a). For the heterostructure Si(p)/TPyP/Si(p) with identical p type Si electrodes (high resistivity: 3.08 Ωcm) a blocking effect of the contact was not evidenced . The contact is injector and the space charge limitation appeared at voltages > 1 V (Fig. 6 b) independent of polarization. The same behavior has been obtained for the heterostructure with p type Si electrodes of different resistivity (0.075 Ωcm and 3.08 Ωcm). The charge carrier injection is determined by the energetic barrier at the contact Si/TPyP. The energetic barrier at the contact Si(n)/TPyP between the energetic level of the electrons in n type Si (4 eV) and LUMO level in TPyP (4.1 eV [18]) is ΔE~0.1 eV much lower that the energetic barrier at the contact Si(p)/TPyP between the energetic level of holes in p type Si (5.1 eV) and the HOMO level in TPyP (6.8 eV [19]), ΔE=1.7 eV. On the other hand, the current is higher in the heterostructures prepared with n type Si because of the charge carrier scattering is lower in the layer with larger grain morphology (Table 1).

A blocking behaviour has been also evidenced for asymmetric Si electrodes heterostructures Si(n)/TPyP/Si(p) at direct polarization for both type of Si anode (Fig. 6 c and d).

A steep increase in the current for an applied voltage < 1V has been obtained for the low resistivity Si anode (0.075 Ωcm) because it is favored the injection of the charge carriers from the lower resistivity p type silicon (Fig. 6 e). For heterostructures with high resitivity Si anode was evidenced a mostly linear characteristic at low voltages (<0.1 V) and a power dependence with n=3 that correspond to the trap charge limited currents at voltages > 1 V (Fig. 6 f).

The heterostructure realized with ITO and n (Fig. 7 a) or p (Fig. 7 b) type Si electrodes have a blocking diode behavior at both direct and reverse bias at low voltages (Fig. 7 b) and don't show photoelectric effect.

The I-V characteristics are quasi-linear at low voltages and the limitation by space charge and/or trap charge of the currents became important at higher voltages.

The conduction of the TPyP layer grown on ITO substrate is lower because the smaller grain morphology favors the charge carrier scattering on the grain boundaries.

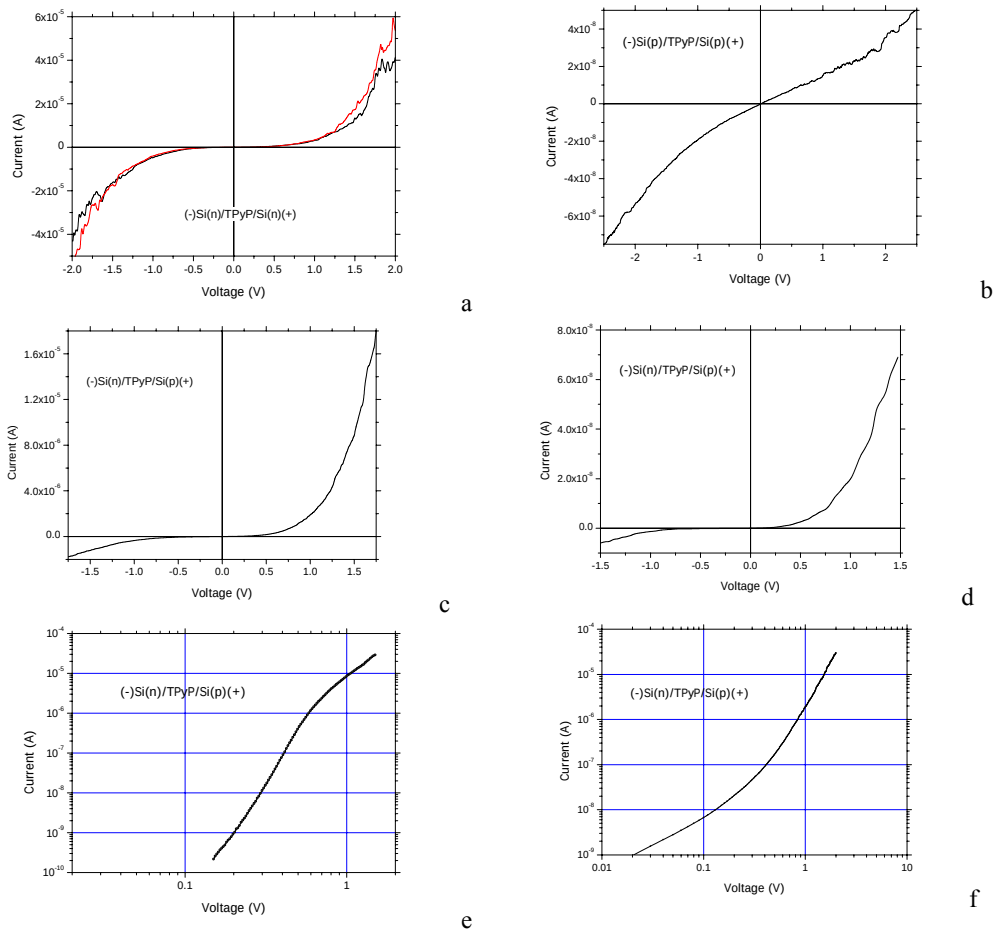

Fig. 6. I-V characteristics for different type of heterostructures realized with Si electrodes: (a) Si(n)/TPyP/Si(n); (b) Si(p)/TPyP/Si(p); (c) Si(n)/TPyP/Si(p, 3.08Ωcm); (d) Si(n)/TPyP/Si(p,0.075Ωcm); (e) Si(n)/TPyP/Si(p, 3.08 Ωcm);(detail); (f) Si(n)/TPyP/Si(p, 0.075 Ωcm), detail.

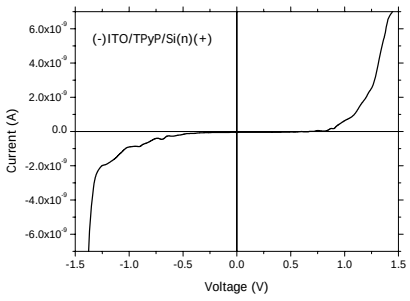

a

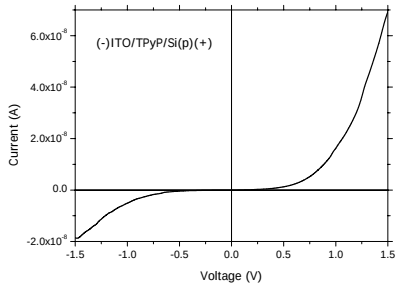

b

Fig. 7. I-V characteristics for different type of heterostructures realized with Si and ITO electrodes: (a) ITO/TPyP/Si(n); (b); ITO/TPyP/Si(p).

A blocking contact between ITO and TPyP has been previously mentioned in heterostructure ITO/TPyP/Al [20].

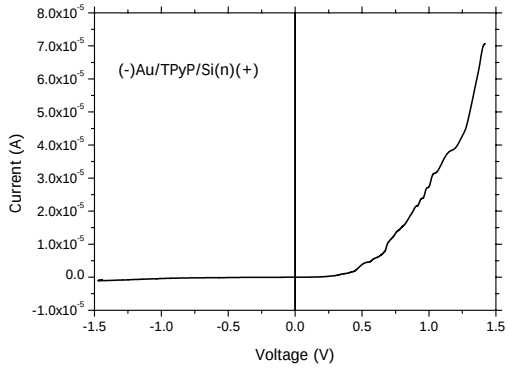

Fig. 8. I-V characteristic for a heterostructure realized with metallic electrode.

A rectifier behavior has been evidenced for Au/TPyP/Si(n) heterostructure at direct polarization (Au electode is cathode and Si(n) is anode). This behavior is favored by the lowering of the energetic barrier at the contact Au/TPyP (Au work function (ϕ)=5.1 eV and $LUMO_{TPyP}$=4.1 eV) by applying a voltage higher than 0.30 eV. At very low voltages the I-V characteristic is linear and becomes a power dependence with n>2 corresponding to trap charge limited current limitation at voltages >0.1 V. A blocking behavior appeared for the same heterostructure at reverse bias (Fig. 8), independently of the applied voltage because the charge carriers can not surpass the energetic contact barrier.

4. Conclusions

We have investigated the optical and electrical properties of the TPyP films deposited by vacuum evaporation on different substrates The UV-Vis transmission spectra have evidenced a structured shape of the transmission curve in the domain ranging from 200 nm to 800 nm with an intense Soret band (B) with a peak around 430 nm and 4 Q bands situated at 520 nm, 555 nm, 590 nm and 645 nm. The shape of the absorption spectra of the thin films deposited by vacuum evaporation on different substrates is preserved for wavelengths > 430 nm but some differences (a less structured Soret band and weak UV absorption peak around 330 nm) have been evidenced for TPyP film deposited on ITO covered glass. The interaction between the molecules in the solid state determines the slight red shift of the B band. This behavior can be correlated with the particularities of the individual molecules and of the connection existing between the molecules in the vacuum deposited layer.

The similarity between the FTIR spectra of solid state TPyP and of powder TPyP in BrK mixture and the photoluminescence spectra of TPyP films deposited on Si which have revealed two emission Q bands situated at 660 nm and 710 nm which correspond to free base TPyP, confirm that by vacuum evaporation the chemical structure is preserved, vacuum evaporation being an adequate method for the preparation of TPyP thin films. The grain morphology of the vacuum deposited layers has been revealed by AFM with the larger grain dimension for TPyP deposited on Si(n) and the lower dimension for TPyP film deposited on quartz. This morphology sustains a higher value of the currents injected in the heterostructures realized with n type Si and a lower optical scattering in the TPyP layers deposited on quartz. Most of the heterostructures ITO (Si)/TPyP/Si have a blocking behavior both for n type and p type Si. The only rectifier behavior was emphasized for Au/TPyP/Si(n) heterostructure.

Acknowledgment

This research was financially supported by the Romanian Ministry of Education and Research through National Core Founding Program, Contract No: 45N/27.02.2009.

References

[1] C. M. Drain, Proc. Natl. Acad. Sci. U.S.A. **99**, 5178 (2002).
[2] E. Fagadar-Cosma, C. Enache, I. Armeanu, G. Fagadar-Cosma, Digest Journal of Nanomaterials

and Biostructures **2**, 175 (2007).
[3] S. R. Forrest, Chem. Rev. **97**, 1793 (1997).
[4] H. George, Q. Guo, J. Phys.: Conference Series **100**, 1 (2008).
[5] W. Auwärter, A. Weber-Bargioni, A. Riemann, A. Schiffrin, O. Gröning, R. Fasel, J. V. Barth, J. Chem. Phys. **124**, 194708/1 (2006).
[6] T. Yokoyama, S. Yokoyama, T. Kamikado, S. Mashiko, J. Chem. Phys. **115**, 3814 (2001).
[7] J. A. Shelnutt, X.-Z. Song, J.-G. Ma, S.-L. Jia, W. Jentzen, C. J. Medforth, Chem. Soc. Rev **27**, 31 (1998).
[8] R. L. Lader, E. J. Heider, M. F. Perutz, J. Mol. Biol. **114**, 385 (1977).
[9] M. K. Geno, J. Hallepern, J. Am. Chem. Soc. **109**, 1238 (1987).
[10] A. Stanculescu, F. Stanculescu, L. Tugulea, M. Socol, Mat. Sci. Forum **514-516**, 956 (2006).
[11] A. Stanculescu, F. Stanculescu, Thin Solid Films, **515**, 8733 (2007).
[12] D. Dolphin (Ed.) The Porphyrins, vols 1-7, Academic Press, New York (1978).
[13] M. M. El-Nahass, H. M. Zeyada, M. S. Aziz, M. M. Makhouf, Spectrochimica Acta Part A: Molecular and Biomolecular spectroscopy, **61**, 3026 (2005).
[14] F. Klappenberger, A. Weber-Bargioni, W. Auwärter, M. Marschall, A. Schiffrin, J. V. Barth, J. Chem. Phys. **129**, 214702/1 (2008).
[15] W. Auwärter, F. Klappenberger, A. Weber-Bargioni, A. Schiffrin, T. Strunskus, C. Wöll, Y. Pennec, A. Riemann, J. V. Barth, J. Am. Chem. Soc. **129**, 11279 (2007).
[16] C. Guillén, J. Herrero, Thin Solid Films **480-481**, 129 (2005).
[17] S. K. Park, J. I. Han, W. K. Kim, M. G. Kwak, Thin Solid Films, **397**, 49 (2001).
[18] Stefan Antohe, Chapter 11 „Electronic and Optoelectronic Devices Based on Organic Thin Films" in Handbook of Organic Electronics and Photonics (Electronic Materials and Devices), Edited by Hari Singh Nalwa p. 435 American Scientific Publishers (2008).
[19] O.-L. Rasoga, M. Socol, F. Stanculescu, J. Optoelectron. Adv. Mater. **11**(4), 509 (2009).
[20] S. Antohe, Phys. Stat. Sol. (a) **136**, 401 (2006).

*Corresponding author: cela@infim.ro